

# Azimuthal Anisotropy in U+U and Au+Au Collisions at RHIC

---

(STAR Collaboration) Adamczyk, L.; ...; Planinić, Mirko; ...; Poljak, Nikola; ...; Zyzak, M.

Source / Izvornik: **Physical Review Letters, 2015, 115**

Journal article, Published version

Rad u časopisu, Objavljena verzija rada (izdavačev PDF)

<https://doi.org/10.1103/PhysRevLett.115.222301>

Permanent link / Trajna poveznica: <https://urn.nsk.hr/urn:nbn:hr:217:752329>

Rights / Prava: [In copyright](#)

Download date / Datum preuzimanja: **2020-12-03**



Repository / Repozitorij:

[Repository of Faculty of Science - University of Zagreb](#)



## Azimuthal Anisotropy in U + U and Au + Au Collisions at RHIC

L. Adamczyk,<sup>1</sup> J. K. Adkins,<sup>20</sup> G. Agakishiev,<sup>18</sup> M. M. Aggarwal,<sup>30</sup> Z. Ahammed,<sup>47</sup> I. Alekseev,<sup>16</sup> J. Alford,<sup>19</sup> A. Aparin,<sup>18</sup> D. Arkhipkin,<sup>3</sup> E. C. Aschenauer,<sup>3</sup> G. S. Averichev,<sup>18</sup> A. Banerjee,<sup>47</sup> R. Bellwied,<sup>43</sup> A. Bhasin,<sup>17</sup> A. K. Bhati,<sup>30</sup> P. Bhattarai,<sup>42</sup> J. Bielcik,<sup>10</sup> J. Bielcikova,<sup>11</sup> L. C. Bland,<sup>3</sup> I. G. Bordyuzhin,<sup>16</sup> J. Bouchet,<sup>19</sup> A. V. Brandin,<sup>26</sup> I. Bunzarov,<sup>18</sup> T. P. Burton,<sup>3</sup> J. Butterworth,<sup>36</sup> H. Caines,<sup>51</sup> M. Calderón de la Barca Sánchez,<sup>5</sup> J. M. Campbell,<sup>28</sup> D. Cebra,<sup>5</sup> M. C. Cervantes,<sup>41</sup> I. Chakaberia,<sup>3</sup> P. Chaloupka,<sup>10</sup> Z. Chang,<sup>41</sup> S. Chattopadhyay,<sup>47</sup> J. H. Chen,<sup>39</sup> X. Chen,<sup>22</sup> J. Cheng,<sup>44</sup> M. Cherney,<sup>9</sup> W. Christie,<sup>3</sup> G. Contin,<sup>23</sup> H. J. Crawford,<sup>4</sup> S. Das,<sup>13</sup> L. C. De Silva,<sup>9</sup> R. R. Debbé,<sup>3</sup> T. G. Dedovich,<sup>18</sup> J. Deng,<sup>38</sup> A. A. Derevschikov,<sup>32</sup> B. di Ruzza,<sup>3</sup> L. Didenko,<sup>3</sup> C. Dilks,<sup>31</sup> X. Dong,<sup>23</sup> J. L. Drachenberg,<sup>46</sup> J. E. Draper,<sup>5</sup> C. M. Du,<sup>22</sup> L. E. Dunkelberger,<sup>6</sup> J. C. Dunlop,<sup>3</sup> L. G. Efimov,<sup>18</sup> J. Engelage,<sup>4</sup> G. Eppley,<sup>36</sup> R. Esha,<sup>6</sup> O. Evdokimov,<sup>8</sup> O. Eyser,<sup>3</sup> R. Fatemi,<sup>20</sup> S. Fazio,<sup>3</sup> P. Federic,<sup>11</sup> J. Fedorisin,<sup>18</sup> Z. Feng,<sup>7</sup> P. Filip,<sup>18</sup> Y. Fisyak,<sup>3</sup> C. E. Flores,<sup>5</sup> L. Fulek,<sup>1</sup> C. A. Gagliardi,<sup>41</sup> D. Garand,<sup>33</sup> F. Geurts,<sup>36</sup> A. Gibson,<sup>46</sup> M. Girard,<sup>48</sup> L. Greiner,<sup>23</sup> D. Grosnick,<sup>46</sup> D. S. Gunarathne,<sup>40</sup> Y. Guo,<sup>37</sup> S. Gupta,<sup>17</sup> A. Gupta,<sup>17</sup> W. Guryn,<sup>3</sup> A. Hamad,<sup>19</sup> A. Hamed,<sup>41</sup> R. Haque,<sup>27</sup> J. W. Harris,<sup>51</sup> L. He,<sup>33</sup> S. Heppelmann,<sup>3</sup> S. Heppelmann,<sup>31</sup> A. Hirsch,<sup>33</sup> G. W. Hoffmann,<sup>42</sup> D. J. Hofman,<sup>8</sup> S. Horvat,<sup>51</sup> H. Z. Huang,<sup>6</sup> B. Huang,<sup>8</sup> X. Huang,<sup>44</sup> P. Huck,<sup>7</sup> T. J. Humanic,<sup>28</sup> G. Igo,<sup>6</sup> W. W. Jacobs,<sup>15</sup> H. Jang,<sup>21</sup> K. Jiang,<sup>37</sup> E. G. Judd,<sup>4</sup> S. Kabana,<sup>19</sup> D. Kalinkin,<sup>16</sup> K. Kang,<sup>44</sup> K. Kauder,<sup>49</sup> H. W. Ke,<sup>3</sup> D. Keane,<sup>19</sup> A. Kechechyan,<sup>18</sup> Z. H. Khan,<sup>8</sup> D. P. Kikola,<sup>48</sup> I. Kisel,<sup>12</sup> A. Kisel,<sup>48</sup> D. D. Koetke,<sup>46</sup> T. Kollegger,<sup>12</sup> L. K. Kosarzewski,<sup>48</sup> L. Kotchenda,<sup>26</sup> A. F. Kraishan,<sup>40</sup> P. Kravtsov,<sup>26</sup> K. Krueger,<sup>2</sup> I. Kulakov,<sup>12</sup> L. Kumar,<sup>30</sup> R. A. Kycia,<sup>29</sup> M. A. C. Lamont,<sup>3</sup> J. M. Landgraf,<sup>3</sup> K. D. Landry,<sup>6</sup> J. Lauret,<sup>3</sup> A. Lebedev,<sup>3</sup> R. Lednicky,<sup>18</sup> J. H. Lee,<sup>3</sup> W. Li,<sup>39</sup> Y. Li,<sup>44</sup> C. Li,<sup>37</sup> Z. M. Li,<sup>7</sup> X. Li,<sup>40</sup> X. Li,<sup>3</sup> M. A. Lisa,<sup>28</sup> F. Liu,<sup>7</sup> T. Ljubicic,<sup>3</sup> W. J. Llope,<sup>49</sup> M. Lomnitz,<sup>19</sup> R. S. Longacre,<sup>3</sup> X. Luo,<sup>7</sup> L. Ma,<sup>39</sup> R. Ma,<sup>3</sup> Y. G. Ma,<sup>39</sup> G. L. Ma,<sup>39</sup> N. Magdy,<sup>50</sup> R. Majka,<sup>51</sup> A. Manion,<sup>23</sup> S. Margetis,<sup>19</sup> C. Markert,<sup>42</sup> H. Masui,<sup>23</sup> H. S. Matis,<sup>23</sup> D. McDonald,<sup>43</sup> K. Meehan,<sup>5</sup> N. G. Minaev,<sup>32</sup> S. Mioduszewski,<sup>41</sup> B. Mohanty,<sup>27</sup> M. M. Mondal,<sup>41</sup> D. A. Morozov,<sup>32</sup> M. K. Mustafa,<sup>23</sup> B. K. Nandi,<sup>14</sup> Md. Nasim,<sup>6</sup> T. K. Nayak,<sup>47</sup> G. Nigmatkulov,<sup>26</sup> L. V. Nogach,<sup>32</sup> S. Y. Noh,<sup>21</sup> J. Novak,<sup>25</sup> S. B. Nurushev,<sup>32</sup> G. Odyniec,<sup>23</sup> A. Ogawa,<sup>3</sup> K. Oh,<sup>34</sup> V. Okorokov,<sup>26</sup> D. L. Olivitt, Jr.,<sup>40</sup> B. S. Page,<sup>3</sup> R. Pak,<sup>3</sup> Y. X. Pan,<sup>6</sup> Y. Pandit,<sup>8</sup> Y. Panebratsev,<sup>18</sup> B. Pawlik,<sup>29</sup> H. Pei,<sup>7</sup> C. Perkins,<sup>4</sup> A. Peterson,<sup>28</sup> P. Pile,<sup>3</sup> M. Planinic,<sup>52</sup> J. Pluta,<sup>48</sup> N. Poljak,<sup>52</sup> K. Poniatowska,<sup>48</sup> J. Porter,<sup>23</sup> M. Posik,<sup>40</sup> A. M. Poskanzer,<sup>23</sup> N. K. Pruthi,<sup>30</sup> J. Putschke,<sup>49</sup> H. Qiu,<sup>23</sup> A. Quintero,<sup>19</sup> S. Ramachandran,<sup>20</sup> S. Raniwala,<sup>35</sup> R. Raniwala,<sup>35</sup> R. L. Ray,<sup>42</sup> H. G. Ritter,<sup>23</sup> J. B. Roberts,<sup>36</sup> O. V. Rogachevskiy,<sup>18</sup> J. L. Romero,<sup>5</sup> A. Roy,<sup>47</sup> L. Ruan,<sup>3</sup> J. Rusnak,<sup>11</sup> O. Rusnakova,<sup>10</sup> N. R. Sahoo,<sup>41</sup> P. K. Sahu,<sup>13</sup> I. Sakrejda,<sup>23</sup> S. Salur,<sup>23</sup> J. Sandweiss,<sup>51</sup> A. Sarkar,<sup>14</sup> J. Schambach,<sup>42</sup> R. P. Scharenberg,<sup>33</sup> A. M. Schmah,<sup>23</sup> W. B. Schmidke,<sup>3</sup> N. Schmitz,<sup>24</sup> J. Seger,<sup>9</sup> P. Seyboth,<sup>24</sup> N. Shah,<sup>6</sup> E. Shaliev,<sup>18</sup> P. V. Shanmuganathan,<sup>19</sup> M. Shao,<sup>37</sup> B. Sharma,<sup>30</sup> M. K. Sharma,<sup>17</sup> W. Q. Shen,<sup>39</sup> S. S. Shi,<sup>7</sup> Q. Y. Shou,<sup>39</sup> E. P. Sichtermann,<sup>23</sup> R. Sikora,<sup>1</sup> M. Simko,<sup>11</sup> M. J. Skoby,<sup>15</sup> D. Smirnov,<sup>3</sup> N. Smirnov,<sup>51</sup> L. Song,<sup>43</sup> P. Sorensen,<sup>3</sup> H. M. Spinka,<sup>2</sup> B. Srivastava,<sup>33</sup> T. D. S. Stanislaus,<sup>46</sup> M. Stepanov,<sup>33</sup> R. Stock,<sup>12</sup> M. Strikhanov,<sup>26</sup> B. Stringfellow,<sup>33</sup> M. Sumbera,<sup>11</sup> B. J. Summa,<sup>31</sup> X. Sun,<sup>23</sup> X. M. Sun,<sup>7</sup> Z. Sun,<sup>22</sup> Y. Sun,<sup>37</sup> B. Surrow,<sup>40</sup> D. N. Svirida,<sup>16</sup> M. A. Szelezniak,<sup>23</sup> Z. Tang,<sup>37</sup> A. H. Tang,<sup>3</sup> T. Tarnowsky,<sup>25</sup> A. N. Tawfik,<sup>50</sup> J. H. Thomas,<sup>23</sup> A. R. Timmins,<sup>43</sup> D. Tlusty,<sup>11</sup> M. Tokarev,<sup>18</sup> S. Trentalange,<sup>6</sup> R. E. Tribble,<sup>41</sup> P. Tribedy,<sup>47</sup> S. K. Tripathy,<sup>13</sup> B. A. Trzeciak,<sup>10</sup> O. D. Tsai,<sup>6</sup> T. Ullrich,<sup>3</sup> D. G. Underwood,<sup>2</sup> I. Upsal,<sup>28</sup> G. Van Buren,<sup>3</sup> G. van Nieuwenhuizen,<sup>3</sup> M. Vandenbroucke,<sup>40</sup> R. Varma,<sup>14</sup> A. N. Vasiliev,<sup>32</sup> R. Vertesi,<sup>11</sup> F. Videbaek,<sup>3</sup> Y. P. Viyogi,<sup>47</sup> S. Vokal,<sup>18</sup> S. A. Voloshin,<sup>49</sup> A. Vossen,<sup>15</sup> F. Wang,<sup>33</sup> Y. Wang,<sup>44</sup> H. Wang,<sup>3</sup> J. S. Wang,<sup>22</sup> Y. Wang,<sup>7</sup> G. Wang,<sup>6</sup> G. Webb,<sup>3</sup> J. C. Webb,<sup>3</sup> L. Wen,<sup>6</sup> G. D. Westfall,<sup>25</sup> H. Wieman,<sup>23</sup> S. W. Wissink,<sup>15</sup> R. Witt,<sup>45</sup> Y. F. Wu,<sup>7</sup> Z. Xiao,<sup>44</sup> W. Xie,<sup>33</sup> K. Xin,<sup>36</sup> Y. F. Xu,<sup>39</sup> N. Xu,<sup>23</sup> Z. Xu,<sup>3</sup> Q. H. Xu,<sup>38</sup> H. Xu,<sup>22</sup> Y. Yang,<sup>7</sup> Y. Yang,<sup>22</sup> C. Yang,<sup>37</sup> S. Yang,<sup>37</sup> Q. Yang,<sup>37</sup> Z. Ye,<sup>8</sup> P. Yepes,<sup>36</sup> L. Yi,<sup>33</sup> K. Yip,<sup>3</sup> I.-K. Yoo,<sup>34</sup> N. Yu,<sup>7</sup> H. Zbroszczyk,<sup>48</sup> W. Zha,<sup>37</sup> X. P. Zhang,<sup>44</sup> J. B. Zhang,<sup>7</sup> J. Zhang,<sup>22</sup> Z. Zhang,<sup>39</sup> S. Zhang,<sup>39</sup> Y. Zhang,<sup>37</sup> J. L. Zhang,<sup>38</sup> F. Zhao,<sup>6</sup> J. Zhao,<sup>7</sup> C. Zhong,<sup>39</sup> L. Zhou,<sup>37</sup> X. Zhu,<sup>44</sup> Y. Zoukarnieva,<sup>18</sup> and M. Zyzak<sup>12</sup>

(STAR Collaboration)

<sup>1</sup>AGH University of Science and Technology, Cracow 30-059, Poland

<sup>2</sup>Argonne National Laboratory, Argonne, Illinois 60439, USA

<sup>3</sup>Brookhaven National Laboratory, Upton, New York 11973, USA

<sup>4</sup>University of California, Berkeley, California 94720, USA

<sup>5</sup>University of California, Davis, California 95616, USA

<sup>6</sup>University of California, Los Angeles, California 90095, USA

- <sup>7</sup>Central China Normal University (HZNU), Wuhan 430079, China  
<sup>8</sup>University of Illinois at Chicago, Chicago, Illinois 60607, USA  
<sup>9</sup>Creighton University, Omaha, Nebraska 68178, USA  
<sup>10</sup>Czech Technical University in Prague, FNSPE, Prague, 115 19, Czech Republic  
<sup>11</sup>Nuclear Physics Institute AS CR, 250 68 Řež/Prague, Czech Republic  
<sup>12</sup>Frankfurt Institute for Advanced Studies FIAS, Frankfurt 60438, Germany  
<sup>13</sup>Institute of Physics, Bhubaneswar 751005, India  
<sup>14</sup>Indian Institute of Technology, Mumbai 400076, India  
<sup>15</sup>Indiana University, Bloomington, Indiana 47408, USA  
<sup>16</sup>Alikhanov Institute for Theoretical and Experimental Physics, Moscow 117218, Russia  
<sup>17</sup>University of Jammu, Jammu 180001, India  
<sup>18</sup>Joint Institute for Nuclear Research, Dubna 141 980, Russia  
<sup>19</sup>Kent State University, Kent, Ohio 44242, USA  
<sup>20</sup>University of Kentucky, Lexington, Kentucky, 40506-0055, USA  
<sup>21</sup>Korea Institute of Science and Technology Information, Daejeon 305-701, Korea  
<sup>22</sup>Institute of Modern Physics, Lanzhou 730000, China  
<sup>23</sup>Lawrence Berkeley National Laboratory, Berkeley, California 94720, USA  
<sup>24</sup>Max-Planck-Institut für Physik, Munich 80805, Germany  
<sup>25</sup>Michigan State University, East Lansing, Michigan 48824, USA  
<sup>26</sup>Moscow Engineering Physics Institute, Moscow 115409, Russia  
<sup>27</sup>National Institute of Science Education and Research, Bhubaneswar 751005, India  
<sup>28</sup>Ohio State University, Columbus, Ohio 43210, USA  
<sup>29</sup>Institute of Nuclear Physics PAN, Cracow 31-342, Poland  
<sup>30</sup>Panjab University, Chandigarh 160014, India  
<sup>31</sup>Pennsylvania State University, University Park, Pennsylvania 16802, USA  
<sup>32</sup>Institute of High Energy Physics, Protvino 142281, Russia  
<sup>33</sup>Purdue University, West Lafayette, Indiana 47907, USA  
<sup>34</sup>Pusan National University, Pusan 609735, Republic of Korea  
<sup>35</sup>University of Rajasthan, Jaipur 302004, India  
<sup>36</sup>Rice University, Houston, Texas 77251, USA  
<sup>37</sup>University of Science and Technology of China, Hefei 230026, China  
<sup>38</sup>Shandong University, Jinan, Shandong 250100, China  
<sup>39</sup>Shanghai Institute of Applied Physics, Shanghai 201800, China  
<sup>40</sup>Temple University, Philadelphia, Pennsylvania 19122, USA  
<sup>41</sup>Texas A&M University, College Station, Texas 77843, USA  
<sup>42</sup>University of Texas, Austin, Texas 78712, USA  
<sup>43</sup>University of Houston, Houston, Texas 77204, USA  
<sup>44</sup>Tsinghua University, Beijing 100084, China  
<sup>45</sup>United States Naval Academy, Annapolis, Maryland 21402, USA  
<sup>46</sup>Valparaiso University, Valparaiso, Indiana 46383, USA  
<sup>47</sup>Variable Energy Cyclotron Centre, Kolkata 700064, India  
<sup>48</sup>Warsaw University of Technology, Warsaw 00-661, Poland  
<sup>49</sup>Wayne State University, Detroit, Michigan 48201, USA  
<sup>50</sup>World Laboratory for Cosmology and Particle Physics (WLCAPP), Cairo 11571, Egypt  
<sup>51</sup>Yale University, New Haven, Connecticut 06520, USA  
<sup>52</sup>University of Zagreb, Zagreb HR-10002, Croatia

(Received 28 May 2015; revised manuscript received 14 October 2015; published 24 November 2015)

Collisions between prolate uranium nuclei are used to study how particle production and azimuthal anisotropies depend on initial geometry in heavy-ion collisions. We report the two- and four-particle cumulants,  $v_2\{2\}$  and  $v_2\{4\}$ , for charged hadrons from U + U collisions at  $\sqrt{s_{NN}} = 193$  GeV and Au + Au collisions at  $\sqrt{s_{NN}} = 200$  GeV. Nearly fully overlapping collisions are selected based on the energy deposited by spectators in zero degree calorimeters (ZDCs). Within this sample, the observed dependence of  $v_2\{2\}$  on multiplicity demonstrates that ZDC information combined with multiplicity can preferentially select different overlap configurations in U + U collisions. We also show that  $v_2$  vs multiplicity can be better described by models, such as gluon saturation or quark participant models, that eliminate the dependence of the multiplicity on the number of binary nucleon-nucleon collisions.

Collisions of nuclei at the Relativistic Heavy-Ion Collider (RHIC) and the Large Hadron Collider (LHC) create a fireball hot and dense enough to form a quark gluon plasma (QGP) [1]. Anisotropies in the final momentum space distributions can be traced back to spatial anisotropies in the initial state and are used to understand the nature of the fireball [2,3]. These anisotropies are studied using harmonics of the distribution of the azimuthal angle  $\phi$  separation between pairs of particles [4–6]. The inference of the properties of the fireball from these measurements is limited however by uncertainties in the description of the initial state [7]. Collisions between uranium nuclei, which have an intrinsic prolate shape [8], provide a way to manipulate this initial geometry to test our understanding of the initial state of heavy-ion collisions and the subsequent fireball [9].

Even in nearly fully overlapping collisions of U nuclei (impact parameter  $b \approx 0$  fm), the initial matter distribution can exhibit very different shapes. In one extreme, the major axes of both colliding nuclei could lie parallel to the beam so that the tip of one nucleus impinges on the tip of the other (tip-tip). Another extreme occurs if the major axes of the nuclei are parallel to each other but perpendicular to the beam so that they collide side-on-side or body-body. There are two principal differences in these two configurations—tip-tip collisions have a larger number of binary nucleon-nucleon collisions  $N_{\text{bin}}$  while body-body collisions have a smaller  $N_{\text{bin}}$  but a more elliptic overlap region (larger eccentricity  $\epsilon_2$ ). The larger  $N_{\text{bin}}$  in the tip-tip configuration is expected to lead to a larger multiplicity of produced particles [10,11] while the more elliptic shape of the body-body collisions is expected to lead to a larger second harmonic anisotropy  $v_2$ . The dependence of  $v_2$  on multiplicity in nearly fully overlapping U + U collisions therefore tests our understanding of particle production and the development of  $v_2$ . An anticorrelation between  $v_2$  and multiplicity in these collisions will also demonstrate that multiplicity can be used to select enhanced samples of body-body or tip-tip configurations. Those samples can then be used to study other topics like the path-length dependence of jet quenching [9], or the extent to which three-particle charge-dependent correlations [12,13] can be attributed to local parity violation [14] or background effects [15]. We also investigate two models that do not include any explicit dependence on  $N_{\text{bin}}$ : one based on gluon saturation [16,17] and the other based on the number of participating constituent quarks [18,19].

In this Letter, we report measurements of the two- and four-particle cumulant of  $v_2$  ( $v_2\{2\}$  and  $v_2\{4\}$ ) in  $^{197}\text{Au} + ^{197}\text{Au}$  and  $^{238}\text{U} + ^{238}\text{U}$  collisions at  $\sqrt{s_{\text{NN}}} = 200$  and 193 GeV, respectively. Both minimum bias and nearly fully overlapping events where most of the nucleons participate in the collision are studied. The data sets were collected by the STAR Collaboration [20] in 2011 and 2012. The U + U data consist of approximately 307 million

events including 7 million specially triggered central events. Charged particles within pseudorapidity window  $|\eta| < 1$  were detected using the STAR time projection chamber (TPC) [21]. We select tracks within the transverse momentum range  $0.2 < p_T < 2.0$  GeV/c. The STAR zero degree calorimeters (ZDCs) [22] were used to select the sample of nearly fully overlapping events, those having large multiplicity but little activity in the ZDCs. The ZDC resolution was determined to be  $23 \pm 2\%$  from the observation of the single neutron peak in the ADC signal. The ZDC selection requires ZDCs on both sides of the detector to have a signal smaller than the specified cut. The tracking efficiency is corrected via embedding and weights in  $\eta$  and  $\phi$  derived from the inverse of the distribution of tracks observed over many events. This method allows us to correct our  $v_2\{2, 4\}$  measurements for imperfections in the tracking efficiency.  $v_2\{4\}$  was calculated using the  $Q$ -cumulant method [23] while  $v_2\{2\}$  was calculated directly from particle pairs  $\langle \cos 2(\phi_1 - \phi_2) \rangle$ . To reduce the contribution from Hanbury Brown and Twiss, Coulomb and track-merging effects, a minimum  $\eta$  separation of  $|\Delta\eta| > 0.1$  is required for  $v_2\{2\}$ . Measurement uncertainties were estimated by varying event and track selection criteria, varying efficiency estimates, and by comparing data from different run periods. These uncertainties are quite small, less than 0.1% absolute variation on  $v_2\{2, 4\}$ .

Figure 1 shows the two- and four-particle cumulant  $v_2\{2\}$  and  $v_2\{4\}$  from minimum bias 200 GeV Au + Au and 193 GeV U + U collisions as a function of efficiency corrected charged particle multiplicity  $dN_{\text{ch}}/d\eta$ . We find that the relationship between  $dN_{\text{ch}}/d\eta$  and centrality fraction can be parameterized as  $(dN_{\text{ch}}/d\eta)^{1/4} = c_1 - c_2x + c_3 \exp(-c_4x^{c_5})$  with  $c_1 = 5.3473$ ,  $c_2 = 4.298$ ,

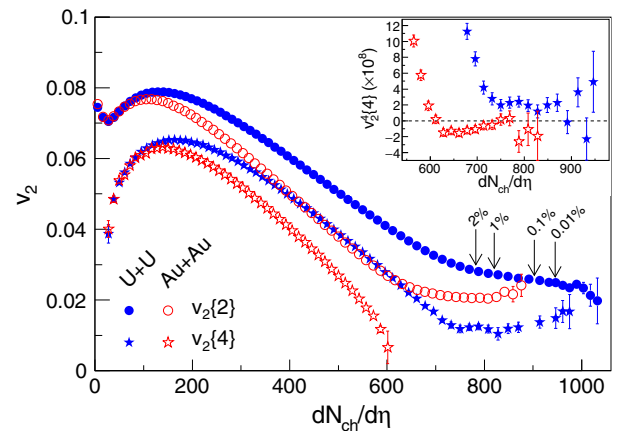


FIG. 1 (color online). The two- and four-particle cumulant  $v_2\{2\}$  and  $v_2\{4\}$  within  $|\eta| < 1$  vs  $dN_{\text{ch}}/d\eta$  from 200 GeV Au + Au and 193 GeV U + U collisions. Dashed lines show U + U centralities based on  $dN_{\text{ch}}/d\eta$  measured in  $|\eta| < 0.5$ .  $v_2^4\{4\}$  (the experimentally observed quantity) is shown in the inset without taking the fourth root in the range where it is near zero or negative.

$c_3 = 0.2959$ ,  $c_4 = 18.21$ , and  $c_5 = 0.4541$  for U + U and  $c_1 = 5.0670$ ,  $c_2 = 3.923$ ,  $c_3 = 0.2310$ ,  $c_4 = 18.37$ , and  $c_5 = 0.4842$  for Au + Au. Multiplicity trends for  $v_2\{2\}$  and  $v_2\{4\}$  in U + U collisions are mostly similar to those observed in Au + Au collisions. A notable difference however is seen in the  $v_2\{4\}$  measurements in central U + U collisions. Whereas  $v_2^4\{4\}$  (shown in the inset) is negative for central Au + Au collisions, it is positive for U + U collisions. Previous studies showed that fluctuations in the number of participating nucleons cause  $v_2^4\{4\}$  in central Au + Au collisions to become negative [24]. The observation of  $v_2^4\{4\} > 0$  in the most central U + U collisions indicates that the prolate shape of uranium increases the anisotropy in the final momentum space distributions of the observed particles.

Glauber-based models have typically used a two-component model  $[(1 - x_{\text{hard}})N_{\text{part}}/2 + x_{\text{hard}}N_{\text{bin}}]$  for the multiplicity, where  $N_{\text{part}}$  is the number of struck nucleons,  $N_{\text{bin}}$  is the number of binary nucleon-nucleon collisions, and  $x_{\text{hard}}$  is a fractional contribution of  $N_{\text{bin}}$  to the multiplicity [10,11]. The multiplicity is then assumed to fluctuate according to a convolution of negative binomial distributions (NBD) with parameters  $n$  and  $k$  related to the mean and width measured from  $p + p$  collisions at the same energy and in the same  $|\eta|$  window [25]. We will refer to this model as ‘‘Glauber- $x_{\text{hard}}$ .’’ Since the number of hard scatterings is known to scale with  $N_{\text{bin}}$ ,  $x_{\text{hard}}$  is often thought of as reflecting the contribution of hard processes to the multiplicity. It can also be thought of as a coherence parameter with  $x_{\text{hard}} = 1$  giving the maximum incoherence as multiplicity entirely arises from independent binary nucleon-nucleon collisions. The Glauber- $x_{\text{hard}}$  model indicates that  $v_2$  in U + U collisions should begin to decrease markedly for events with multiplicities in the top 1% [13] forming a knee structure where tip-tip collisions with larger  $N_{\text{bin}}$  and smaller eccentricity begin to dominate. Vertical dashed lines in the figure indicate the 1%, 0.1%, and 0.01% highest multiplicity U + U collisions. No knee structure is observed suggesting the Glauber- $x_{\text{hard}}$  model may not be the correct description. Adding more multiplicity fluctuations causes the knee structure to disappear [26], but this will also significantly increase the average  $\epsilon_2$  in central collisions.

To explore the dependence of  $v_2$  on the initial eccentricity  $\epsilon_2$ , we plot  $v_2/\epsilon_2$  vs  $dN_{\text{ch}}/d\eta$ . It was found previously that  $v_2/\epsilon_2$  monotonically increases with increasing  $dN_{\text{ch}}/d\eta$  and depending on the model for the initial eccentricity may, or may not saturate in the most central collisions [24]. Figure 2 shows  $v_2\{2\}/\epsilon_2\{2\}$  and  $v_2\{4\}/\epsilon_2\{4\}$  from Au + Au and U + U collisions.  $\epsilon_2\{2\}$  and  $\epsilon_2\{4\}$  are the second and fourth cumulants of the participant eccentricity distributions calculated from the Glauber- $x_{\text{hard}}$  model [27–29]. Both U + U and Au + Au follow a similar trend for  $v_2/\epsilon_2$ . However, a turnover is observed in central collisions ( $dN_{\text{ch}}/d\eta > 500$ ). This has

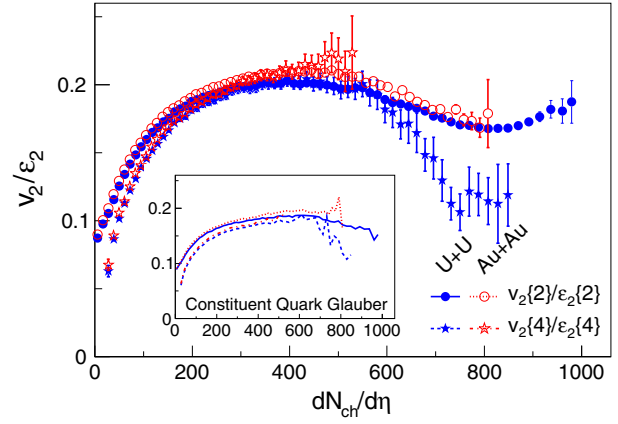


FIG. 2 (color online).  $v_2$  scaled by participant eccentricity from 200 GeV Au + Au and 193 GeV U + U collisions. The eccentricity distributions are calculated in a Monte Carlo Glauber model [27–30]. Both U + U and Au + Au follow a similar trend for  $v_2/\epsilon_2$  and a turnover is observed in central collisions. The inset shows the same quantity but with the eccentricity calculated in a constituent quark Glauber model [18,19] with the Woods-Saxon parameters proposed in Ref. [30].

not been observed previously since measurements have typically been integrated over 5% most central [24]. The turnover is consistent with the model overestimating  $\epsilon_2$  in central collisions. Increasing the multiplicity fluctuations as in Ref. [26] will only increase the eccentricity in central collisions suggesting that a different explanation may be required to explain both the turnover of  $v_2/\epsilon_2$  and the lack of a knee structure in  $v_2$  vs  $dN_{\text{ch}}/d\eta$ . Using a new set of Woods-Saxon parameters derived in Ref. [30] with a smaller diffuseness and smaller deformation parameter  $\beta_2$  in combination with the same Glauber model, reduces the downturn in central U + U collisions somewhat but introduces a mismatch between the U + U and Au + Au curves with the Au + Au curves higher while  $v_2\{4\}/\epsilon_2\{4\}$  for U + U still exhibits a downturn (not shown). In the inset of the figure, we show the result for a new Glauber calculation using constituent quarks as participants [18,19] and the new set of parameters [30]. This estimate for  $\epsilon_2$  leads to a seemingly more natural behavior for  $v_2/\epsilon_2$  with the drop in the highest multiplicity collisions almost entirely gone. The model will be investigated and discussed further below.

The trends of  $v_2$  vs  $dN_{\text{ch}}/d\eta$  are mostly dominated by the elliptic shape of the overlap region in collisions with a nonzero impact parameter. To study body-body or tip-tip collisions, we investigate nearly fully overlapping collisions with minimal activity in the ZDCs. If body-body collisions produce smaller multiplicities than tip-tip collisions, we expect to see a negative slope in  $v_2$  vs multiplicity for these collisions. A negative slope, however, can also come from contamination from larger impact parameter collisions. To assess their contribution, we use collisions of more spherical Au nuclei as a control sample. Figure 3

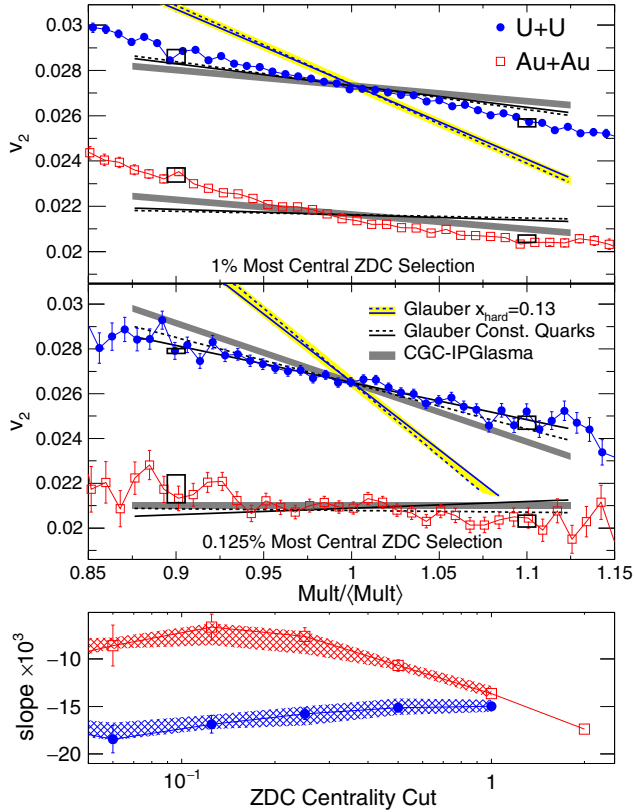


FIG. 3 (color online). Top panels: charged particle  $v_2\{2\}$  vs normalized multiplicity within  $|\eta| < 1.0$ . The upper panel is for the top 1% most central events based on the smallness of the ZDC signal, while the middle panel is for the top 0.125%. Small boxes indicate the possible range of variation of  $v_2$  from uncertainties in the efficiency corrections on the  $x$  axis. Model comparisons are described in the text. Bottom panel: The slopes as a function of increasingly tighter ZDC centrality selections. The systematic uncertainties are shown as bands.

shows the elliptic flow  $v_2\{2\}$  of all charged particles as a function of the normalized multiplicity ( $\text{Mult}/\langle \text{Mult} \rangle$ ) for two different systems. We increase the acceptance to  $|\eta| < 1.0$  to reduce multiplicity fluctuations. The upper panel shows the results for the 1% most central events based on the smallest signal seen in the ZDCs. Both Au + Au and U + U show a negative slope, which indicates the effect of the impact parameter is still prominent (otherwise, we expect the Au + Au slope to be nearly flat or even positive). The middle panel of Fig. 3 shows the 0.125% most central events. The negative slope for Au + Au collisions is smaller in magnitude, indicating the effects from noncentral collisions are reduced and the variation in multiplicity in Au + Au collisions is mainly driven by fluctuations. The bottom panel of Fig. 3 shows how the slopes extracted from  $v_2$  vs normalized multiplicity evolve with successively tighter ZDC sections. While the slope for Au + Au collisions becomes less negative, the slope for U + U collisions becomes steeper as the centrality selection is tightened. This demonstrates that the variation of

multiplicity in the 0.125% U + U collisions is dominated by the different geometries made possible by the prolate shape of the uranium nucleus and that tip-tip collisions produce more multiplicity than body-body collisions. Systematic uncertainties shown as bands on the slope were estimated by varying the fit range and efficiency corrections. Other sources of systematic error are smaller and subdominant compared to the variation due to the range of efficiencies used in the error analysis. Due to large statistical errors, no conclusions could be drawn from studies of  $v_2\{4\}$  vs multiplicity in these events. We also measured  $v_3\{2\}$  in central collisions and found that  $v_3\{2\}$  in the 0.125% most central collisions are  $(1.410 \pm 0.006) \times 10^{-2}$  for U + U and  $(1.380 \pm 0.008) \times 10^{-2}$  in Au + Au collisions (statistical errors only). The slope of  $v_3$  vs multiplicity was small and negative in both systems at about  $-0.005 \pm 0.002$ .

The U + U data in the top panels of Fig. 3 are compared to the Glauber- $x_{\text{hard}}$  model (assuming  $v_2 = \varepsilon_2\langle v_2 \rangle / \langle \varepsilon_2 \rangle$ ). The ZDC response was modeled by calculating the number of spectator neutrons from the Glauber model (accounting for the charge to mass ratio of the nucleus) and folding each neutron with the known ZDC resolution for a single neutron. The Glauber- $x_{\text{hard}}$  model significantly overpredicts the observed slope for U + U. This indicates that the variation in multiplicity between tip-tip collisions and body-body collisions is smaller than anticipated if multiplicity has a significant contribution proportional to  $N_{\text{bin}}$ . Given this failure, we investigate two alternatives with no explicit  $N_{\text{bin}}$  dependence: a constituent-quark Glauber model (Glauber-CQ) [18,19] and the IP-Glasma model [17] based on gluon saturation [16]. The Glauber-CQ model neglects  $N_{\text{bin}}$  and counts the number of participating constituent quarks  $N_{\text{CQ}}$  with each nucleon being treated as three constituent quarks distributed according to  $\rho = \rho_0 \exp(-ar)$  with  $a = 4.27 \text{ fm}^{-1}$  [19]. This model with  $\sigma_{qq} = 9.36 \text{ mb}$  provides a good description of transverse energy and multiplicity distributions at RHIC [19] and a better description of  $v_2$  fluctuations than a nucleon based Glauber model [24]. In our simulation, for each  $N_{\text{CQ}}$ , we sample an NBD with parameters tuned to match the distributions from  $p + p$  [25] and Au + Au at 200 GeV ( $n = 0.76$ , and  $k = 0.34$  for  $|\eta| < 0.5$  and  $n = 2.9$  and  $k = 0.86$  for  $|\eta| < 1$ ). For both Glauber models, we use two sets of parameters for the nuclear geometry, one corresponding to the more commonly used values [29] (dashed lines) and the new parameters proposed in Ref. [30] (solid lines). The effect of the different parameter sets is small. The IP-Glasma and Glauber-CQ model are also compared to the Au + Au data (Glauber- $x_{\text{hard}}$  is left off for clarity) but because of significant uncertainty in the actual shape of a Au nucleus, it is difficult to draw conclusions from this comparison.

In U + U collisions, both the IP-Glasma model and the Glauber-CQ model predict slopes closer to the data. In the

Glauber-CQ model, even though there is no dependence on  $N_{\text{bin}}$ , the average number of quarks struck in a nucleon ( $N_{\text{CQ}}/N_{\text{part}}$ ) is larger in tip-tip than in body-body collisions so that tip-tip collisions create more multiplicity. This leads to a strong anticorrelation between  $N_{\text{CQ}}/N_{\text{part}}$  and  $\varepsilon_2$ , which in turn translates into a negative slope in  $v_2$  vs multiplicity. The IP-Glasma model exhibits similar behavior. In gluon saturation models like the IP-Glasma model, the multiplicity depends on  $Q_s^2 S_{\perp}/\alpha_S(Q_s^2)$  [17], where  $Q_s^2$  (the saturation scale) is determined by the thickness of the nucleus along the beam axis,  $S_{\perp}$  is the transverse size of the overlap region, and  $\alpha_S$  is the strong coupling constant. For tip-tip collisions, the increase in  $Q_s^2$  in the numerator will be balanced by a decrease of  $S_{\perp}$ . In the denominator, however,  $\alpha_S$  decreases logarithmically with  $Q_s^2$  leading to an increased multiplicity in tip-tip collisions compared to body-body collisions.

The slope of  $v_2$  vs multiplicity provides a detailed probe of the multiplicity production mechanism and the degree of coherence in nuclear collisions. We find that accounting for the observed slope seems to require models that include effects from subnucleonic structure and significantly more coherence than is expected from the Glauber- $x_{\text{hard}}$  model. Previous studies questioned the relevance of  $N_{\text{bin}}$  because of the apparent lack of an energy dependence to  $x_{\text{hard}}$  and because the Glauber-CQ model also provides a good description of multiplicity data. This study however, provides direct evidence contradicting the Glauber- $x_{\text{hard}}$  model.

In summary, we measured  $v_2\{2\}$  and  $v_2\{4\}$  for minimum bias, and nearly fully overlapping Au + Au and U + U collisions at  $\sqrt{s_{NN}} = 200$  and 193 GeV, respectively. The knee structure in high multiplicity U + U collisions predicted by a Glauber model with a two component multiplicity model with a dependence on  $N_{\text{bin}}$  is not observed in  $v_2$  vs  $dN_{\text{ch}}/d\eta$ . Also,  $v_2$  scaled by  $\varepsilon_2$  from this model is found to saturate and then decrease for the most central U + U collisions. These findings indicate a weakness in the two-component multiplicity calculation that is commonly used as part of Glauber models in heavy-ion collisions. We also used the STAR ZDCs to select nearly fully overlapping collisions and showed that for a stringent 0.125% ZDC selection criterion, the variation of  $v_2$  with multiplicity in U + U collisions is dominated by the different geometries arising from the prolate shape of the uranium nucleus. This demonstrates that ZDCs and multiplicity can be used to select tip-tip or body-body enriched event samples. The variation of  $v_2$  with multiplicity in nearly fully overlapping collisions was shown to again disfavor the Glauber model including a fractional contribution of  $N_{\text{bin}}$  to multiplicity. Models with no explicit  $N_{\text{bin}}$  dependence such as a gluon saturation based model (IP-Glasma) or a constituent quark Glauber model agree better with the data. In addition to revealing fundamental information about the nature of particle

production in heavy-ion collisions, the findings in this Letter lay the groundwork for more extensive studies of the effect of the initial geometry on other observables in nearly fully overlapping collisions.

We thank the RHIC Operations Group and RCF at BNL, the NERSC Center at LBNL, the KISTI Center in Korea, and the Open Science Grid consortium for providing resources and support. This work was supported in part by the Office of Nuclear Physics within the U.S. DOE Office of Science, the U.S. NSF, the Ministry of Education and Science of the Russian Federation, NNSFC, CAS, MoST and MoE of China, the Korean Research Foundation, GA and MSMT of the Czech Republic, FIAS of Germany, DAE, DST, and UGC of India, the National Science Centre of Poland, National Research Foundation, the Ministry of Science, Education and Sports of the Republic of Croatia, and RosAtom of Russia.

- 
- [1] M. Gyulassy and L. McLerran, *Nucl. Phys.* **A750**, 30 (2005).
  - [2] A. P. Mishra, R. K. Mohapatra, P. S. Saumia, and A. M. Srivastava, *Phys. Rev. C* **77**, 064902 (2008).
  - [3] P. Sorensen, *J. Phys. G* **37**, 094011 (2010); P. Sorensen, B. Bolliet, A. Mocsy, Y. Pandit, and N. Pruthi, *Phys. Lett. B* **705**, 71 (2011).
  - [4] J.-Y. Ollitrault, *Phys. Rev. D* **46**, 229 (1992).
  - [5] K. H. Ackermann *et al.* (STAR Collaboration), *Phys. Rev. Lett.* **86**, 402 (2001); J. Adams *et al.* (STAR Collaboration), *Phys. Rev. Lett.* **92**, 052302 (2004); B. I. Abelev *et al.* (STAR Collaboration), *Phys. Rev. C* **77**, 054901 (2008).
  - [6] J. Adams *et al.* (STAR Collaboration), *Nucl. Phys.* **A757**, 102 (2005); K. Adcox *et al.* (PHENIX Collaboration), *Nucl. Phys.* **A757**, 184 (2005); B. B. Back *et al.*, *Nucl. Phys.* **A757**, 28 (2005); I. Arsene *et al.* (BRAHMS Collaboration), *Nucl. Phys.* **A757**, 1 (2005).
  - [7] T. Hirano, U. W. Heinz, D. Kharzeev, R. Lacey, and Y. Nara, *Phys. Lett. B* **636**, 299 (2006).
  - [8] S. Raman, C. W. G. Nestor, Jr., and P. Tikkannen, *At. Data Nucl. Data Tables* **78**, 1 (2001).
  - [9] U. Heinz and A. Kuhlman, *Phys. Rev. Lett.* **94**, 132301 (2005); A. Kuhlman and U. Heinz, *Phys. Rev. C* **72**, 037901 (2005); A. Kuhlman, U. W. Heinz, and Y. V. Kovchegov, *Phys. Lett. B* **638**, 171 (2006); C. Nepali, G. Fai, and D. Keane, *Phys. Rev. C* **73**, 034911 (2006).
  - [10] D. Kharzeev and M. Nardi, *Phys. Lett. B* **507**, 121 (2001).
  - [11] M. L. Miller, K. Reygers, S. J. Sanders, and P. Steinberg, *Annu. Rev. Nucl. Part. Sci.* **57**, 205 (2007).
  - [12] B. I. Abelev *et al.* (STAR Collaboration), *Phys. Rev. Lett.* **103**, 251601 (2009).
  - [13] S. A. Voloshin, *Phys. Rev. Lett.* **105**, 172301 (2010).
  - [14] D. Kharzeev, *Phys. Lett. B* **633**, 260 (2006).
  - [15] S. Schlichting and S. Pratt, *Phys. Rev. C* **83**, 014913 (2011).
  - [16] L. D. McLerran and R. Venugopalan, *Phys. Rev. D* **49**, 2233 (1994); L. D. McLerran and R. Venugopalan, *Phys. Rev. D* **49**, 3352 (1994).

- [17] B. Schenke, P. Tribedy, and R. Venugopalan, *Phys. Rev. C* **86**, 034908 (2012); B. Schenke, P. Tribedy, and R. Venugopalan, *Phys. Rev. C* **89**, 064908 (2014).
- [18] S. Eremín and S. Voloshin, *Phys. Rev. C* **67**, 064905 (2003).
- [19] S. S. Adler *et al.* (PHENIX Collaboration), *Phys. Rev. C* **89**, 044905 (2014); A. Adare *et al.*, arXiv:1509.06727.
- [20] K. H. Ackermann *et al.* (STAR Collaboration), *Nucl. Instrum. Methods Phys. Res., Sect. A* **499**, 624 (2003).
- [21] M. Anderson *et al.*, *Nucl. Instrum. Methods Phys. Res., Sect. A* **499**, 659 (2003).
- [22] F. S. Bieser *et al.*, *Nucl. Instrum. Methods Phys. Res., Sect. A* **499**, 766 (2003).
- [23] A. Bilandzic, R. Snellings, and S. Voloshin, *Phys. Rev. C* **83**, 044913 (2011); A. Bilandzic, C. H. Christensen, K. Gulbrandsen, A. Hansen, and Y. Zhou, *Phys. Rev. C* **89**, 064904 (2014).
- [24] G. Agakishiev *et al.* (STAR Collaboration), *Phys. Rev. C* **86**, 014904 (2012).
- [25] R. E. Ansorge *et al.* (UA5 Collaboration), *Z. Phys. C* **43**, 357 (1989).
- [26] M. Rybczynski, W. Broniowski, and G. Stefanek, *Phys. Rev. C* **87**, 044908 (2013).
- [27] R. S. Bhalerao and J.-Y. Ollitrault, *Phys. Lett. B* **641**, 260 (2006).
- [28] W. Broniowski, P. Bozek, and M. Rybczynski, *Phys. Rev. C* **76**, 054905 (2007).
- [29] H. Masui, B. Mohanty, and N. Xu, *Phys. Lett. B* **679**, 440 (2009).
- [30] Q. Y. Shou, Y. G. Ma, P. Sorensen, A. H. Tang, F. Videdaek, and H. Wang, *Phys. Lett. B* **749**, 215 (2015).